International Journal of Environmental Research (2021) 15:1–10
https://doi.org/10.1007/s41742-020-00296-9

RESEARCH PAPER

Catalytic Oxidation of Dyeing Wastewater by Copper Oxide Activating Persulfate: Performance, Mechanism and Application

Yuxuan Ye[1,2] · Jun Wan[1,2] · Qiang Li[1,2] · Yangbo Huang[1,2] · Fei Pan[1,2] · Dongsheng Xia[1,2]

Received: 24 July 2020 / Revised: 28 September 2020 / Accepted: 19 October 2020 / Published online: 31 October 2020

Abstract

The effective treatment of dyeing wastewater has been considered as one of the challenges. The sulfate radical ($SO_4^{\bullet-}$)-based technology exhibited great potential in the field of organic wastewater treatment. In this study, copper oxide was synthesized and used to activate persulfate (PS) for removing methylene blue (MB) from aqueous solution. The effects of reaction parameters and coexisting substances on this process were studied. Under the optimal conditions ([CuO] = 0.2 g/L, [PS] = 2 g/L, pH = 7.0–9.0), more than 90% of MB was degraded. Cl^- had little effect on MB removal, while SO_4^{2-} and HCO_3^- showed inhibitory effect. The activation energy of the reaction was 137.8 kJ/mol at 25 ℃ with an initial MB concentration of 10 mg/L. The mechanisms of PS activated by CuO was elucidated by radical scavenger and electron spin resonance trapping studies. The results found that sulfate radical ($SO_4^{\cdot-}$) and singlet oxygen ($^1O_2$) were the primary reactive oxygen species in the CuO/PS system. The recycling experiments showed that MB removal efficiency remained more than 70% after five cycles, which exhibited good stability and high efficiency of the catalyst. The favorable degradation performance of simulated textile wastewater indicated the potential application of CuO/PS for dyeing wastewater treatment.

Article Highlights

- **CuO prepared by hydrothermal method can effectively activate PS to degraded MB.**
- **The optimal degradation conditions was [CuO] = 0.2 g/L, [PS] = 2 g/L, pH = 7.0–9.0.**
- **$SO_4^{\cdot-}$ and $^1O_2$ were the primary reactive species in the CuO/PS system.**
- **MB removal efficiency remained more than 70% after 5 cycles.**

Keywords Catalytic oxidation · Copper oxide · Persulfate · Dyeing wastewater · Mechanism

Introduction

The dyeing industry is one of the seriously water-polluted industries in China. The amount of wastewater generated from such industry is relatively large, and most of the dye in the wastewater is toxic, carcinogenic and hard to be biodegraded (Feng et al. 2012; Li et al. 2019). If dyeing wastewater is discharged without proper treatment, it will bring serious pollution and then pose a threat to human beings (Florenza et al. 2014; Oliveira Cruz et al. 2020; Damasceno et al. 2020). Some methods of treatment technologies have been adopted for the removal of dyes, such as coagulation (Dotto et al. 2019), adsorption (Sayğılı and Güzel 2016), membrane separation (He et al. 2008; Zhan et al. 2018), etc. But there are still some defects. For instance, a large amount of toxic sludge will be produced

Yuxuan Ye and Jun Wan contributed equally to this work and were the co-first authors.

Electronic supplementary material The online version of this article (https://doi.org/10.1007/s41742-020-00296-9) contains supplementary material, which is available to authorized users.

✉ Qiang Li
qiangli@wtu.edu.cn

✉ Dongsheng Xia
dongsheng_xia@wtu.edu.cn

[1] School of Environmental Engineering, Wuhan Textile University, Wuhan 430073, People's Republic of China

[2] Engineering Research Center for Clean Production of Textile Dyeing and Printing, Ministry of Education, Wuhan 430073, People's Republic of China

in the coagulation process (Vijayaraghavan et al. 2011), the preparation of some highly efficient adsorbents is complicated (Sayğılı et al. 2015; Li et al. 2018a), and membrane fouling restricted its large-scale application (Hu and Long 2016). Compared with the above technologies, advanced oxidation has attracted much attention because of its high effectiveness and little pollution (Ghauch et al. 2012a; Liu et al. 2013).

Recently, the sulfate radical ($SO_4\cdot^-$)-based technology exhibited great potential in the field of organic wastewater treatment for a high E_0 value of 2.5–3.1 V (Liu et al. (2012)). $SO_4\cdot^-$ can be produced by activating persulfate (Wacławek et al. 2017; Chen et al. 2017; Oh et al. 2016), and a variety of activation methods were developed, such as heat (Johnson et al. 2008), light (Guan et al. 2011), transition metals (Drzewicz et al. 2012; Anipsitakis and Dionysiou 2014), alkalinity (Furman et al. 2010), activated carbon (Yang et al. 2011; Qin et al. 2018), and some organic matter (Ahmad et al. 2013). Among them, thermal and light activation requires energy, which increases water treatment prices. Although PS activation with the homogeneous catalysts can be high efficiency at room temperature, residual metals or catalysts left will cause serious environmental health risks (Hu et al. 2016; Wang et al. 2019). Heterogeneous solid catalyst for PS activation has exhibited more and more superiority because of its low cost and easy operation (Yu et al. 2020; Liu et al. 2020).

Copper is a common element for transition metals and is widely used in catalyst preparation due to its low cost and material abundancy. Cu^{2+} complexed with organic degradation intermediates can be easily decomposed, and Cu (I) could be oxidized to Cu (II) at circumneutral pH (Huang et al. 2020). Copper oxide has shown advantageous performance on activated PS degradation of pollutants. Zhang et al. showed that the copper oxide can directly activate PS for the degradation of 2, 4-dichlorophenol and found a non-radical process was involved in this reaction (Zhang et al. 2014). Ji et al. reported that a well-crystallized CuO can activate peroxymonosulfate (PMS) for the removal of phenol, the main degradation radicals attributed to sulfate and hydroxyl radicals (Ji et al. 2011). Du et al. found activated persulfate along with trace sulfate and hydroxyl radicals were reactive oxygen species in copper oxide activated persulfate system, activated persulfate was predominant instead of sulfate and hydroxyl radicals (Du et al. 2017). Liang et al. observed that the degradation of *p*-chloroaniline by the copper oxide possibly occurred in the boundary layer of the copper oxidate surface at the neutral initial pH (Liang et al. 2013). There still exist some problems in the mechanisms of copper oxide activating PS to decolorize and degrade different dyes, especially the leaching of copper in different conditions. Furthermore, the performance and mechanism of using CuO/PS process in dyeing wastewater treatment were also not clear. The reusable and stability of CuO in its application were urgent need to find out.

In this study, CuO was synthesized and used to activate PS for the degradation of organic pollutants. Methylene blue (MB) was selected as the target pollutant. The effect of pH, PS concentration, CuO dosage, MB concentration, inorganic salt concentration, temperature on treatment efficiency were explored. The active species for MB degradation were identified by scavenging experiments and electron paramagnetic resonance (EPR). More importantly, the degradation performance of simulated dyeing wastewater was also verified. This work was expected to provide useful information for the catalytic performance and mechanism of using CuO/PS process in dyeing wastewater treatment.

Materials and Methods

Chemicals and Materials

The chemicals were in analytical grade unless otherwise specified. Methylene blue (MB) and Congo red (CR) were purchased from J&K Chemical Ltd. Sodium persulfate oxidant (PS, $Na_2S_2O_8$, 99%) was purchased from Chem-Lab (China). Chalcanthite ($CuSO_4\cdot5H_2O$, 99%) was provided by Nanjing Chemical Reagent Company (Jiangsu Province, China). NaCl, Na_2SO_4, $NaHCO_3$, HCl, NaOH, methanol (MeOH), tert-butanol (TBA), p-benzoquinone (BQ) and furfuryl alcohol (FFA) were supplied by Sinopharm Chemical Reagent Co., Ltd. (Shanghai, China). 5, 5-Dimethyl-1-pyrroline *N*-oxide (DMPO, 96%) and 2,2,6,6-tetramethyle-4-piperidone (TEMP, 97%) were purchased from Aladdin Reagents Co. Ltd. (Shanghai, China). Aqueous solutions were prepared using deionized water.

Synthesis of CuO Catalysts

The CuO catalyst was prepared by a hydrothermal method. In detail, 6.4 g NaOH was weighed and dissolved in 40 mL deionized water. Then, an aqueous solution of $CuSO_4\cdot5H_2O$ (25%wt, 20 mL) was poured slowly into the aforementioned solution with vigorous stirring. After stirred for 25 min, the produced precipitate was centrifugally separated and washed repeatedly with deionized water and ethanol for three times. Then, it was dried at 90 ℃ for 4 h, and the product was obtained for further use.

Characterizations

XRD (X-ray diffraction) patterns were obtained on a Bruker D8 diffractometer (Bruker-AXS, Karlsruhe, Germany) using filtered Cu Kα radiation ($\lambda = 1.5418^{\circ}$A) with an accelerating voltage of 40 kV and a current of 30 mA. The surface

morphology of the catalyst was observed using a scanning electronic microscope (SEM, S-3400 N II, Hitachi, Japan).

Experimental Process

The catalytic oxidation of MB was carried out in a 250 mL reactor containing 100 mL 10 mg/L of MB solution with a constant stirring at 150 rpm. Unless specifically stated, the reaction temperature was 25℃. When exploring the effect of pH, the initial pH values were adjusted to 1, 3, 5, 7, 9, 10 by 0.1 M NaOH and HCl. 0.02 g CuO catalyst was weighed and added into 100 mL 10 mg/L MB solution, and PS concentrations were 0.1, 0.5, 1.0, 2.0, 4.0, 8.0 g/L, respectively. The residual MB was analyzed at different reaction intervals to explore the best conditions. NaCl, Na_2SO_4 and $NaHCO_3$ were selected to investigate the effect of inorganic salt on degradation. NaCl concentration in reaction system was set as 0, 0.5, 1.0, 2.0, 6.0, 10.0 g/L, respectively, and Na_2SO_4 concentration as 0, 1.0, 2.0, 4.0, 8.0, 10.0 g/L, respectively, and $NaHCO_3$ concentration as 2.0, 4.0, 8.0 g/L, respectively. Temperature's effect on catalytic reaction at 25, 45, 55, 65, 75℃ was explored, respectively, and the activation energy of the reaction was worked out through fitting calculation.

In the quenching experiments, MeOH, TBA, BQ and FFA were adopted to capture free radicals to analyze the main free radicals in the degradation process. 5 min, 10 min, 30 min after the EPR experiment system, 0.2 mL reaction residue liquid was sampled for test. After each reaction, catalysts were washed with deionized water and dried for reuse. 100 mL 10 mg/L MB solution and 0.2 g PS were added to begin the next batch of experiments, and the experiment was repeated for four times. Simulated MB and CR textile wastewater, containing NaCl (4 g/L), $NaHCO_3$ (4 g/L) were prepared. 0.04 g CuO catalyst, 0.2 g PS were added and their catalyze performance were analyzed.

Analytical Methods

UV–Vis spectrophotometer (Varian, USA) was adopted to determine MB absorbance at 664 nm and it was converted into concentration value by standard curve. C/C_0, $(C_0 - C)/C_0$ were adopted in the experiment to characterize the degradation ability of oxidization system for dyes (C_0 was the initial concentration of MB, C was MB concentration at sampling time). The concentration of PS was determined by the potassium iodide method. Free radicals were detected using an electron paramagnetic resonance (EPR) spectrometer (Bruker, A300 Microx). The EPR determination was performed under the following conditions: a centerfield of 3510 G, a microwave power of 18.86 mW, a microwave frequency of 9.854 GHz, a sweep width of 100 G, a modulation frequency of 100 kHz, a receiver gain of 1.0×10^3, modulation amplitude of 1.00 G, a sweep time of 35.84 s. The metal ions were quantified by inductively coupled plasma optical emission spectrometer (ICP-OES, Ultima 2000, Horida).

Results and Discussion

Characterization of CuO Catalyst

The SEM photo showed that the size of the fabricated CuO was at nano-level (Fig. 1a and 1b). The morphology of the catalyst was like rice grains and agglomerated together, and the length was distributed at 200–300 nm. The XRD patterns of the prepared catalyst were shown in Fig. 1c. The peaks of the sample matched well with the standard card of CuO (PDF#80-1916). All the diffraction peaks could be indexed to the monoclinic copper oxide. The result showed a highly crystalline and single-phase structure of CuO, without any peaks of unreacted precursors (Ji et al. 2011). These results

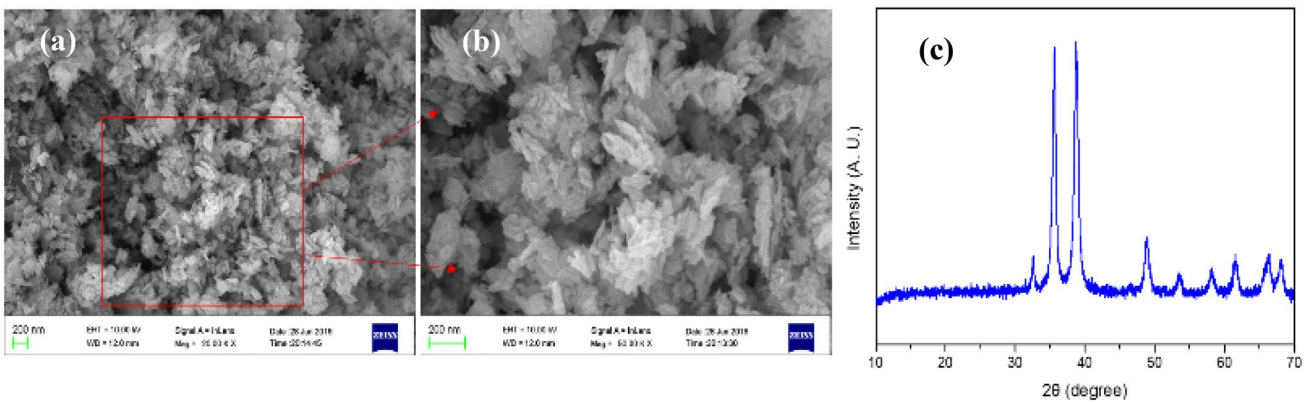

Fig. 1 SEM images (**a**, **b**) and XRD patterns (**c**) of the prepared CuO catalyst

clearly showed that nano-sized CuO was successfully prepared by the simple one-step method.

MB Degradation in Different Conditions

The reaction pH is associated with the protonation degree of PS and charge properties on catalyst surfaces, which affects the catalytic degradation (Wang and Wang 2018). As shown in Fig. 2a, the initial pH of reaction solution played an important role on the removal of MB. The optimum pH for MB degradation was under the initial pH value of 7.0–9.0, and the degradation efficiency was more than 90%. However, the degradation efficiency of MB was suppressed under acidic condition, which may be due to the difficulty in the decomposition of PS under such conditions (Ma et al. 2019). The PS concentration and Cu^{2+} leaching concentration under pHs were monitored, as shown in Fig. 3a and b. It could be seen that the decomposition rate of PS was 12% at pH 3.0, while 90% decomposition rate was achieved at pH 7.0. The poor performance at pH < 7.0 maybe accounted for the low decomposition rate of PS. At the acidic condition, the higher concentration of Cu^{2+} hampered PS decomposition (Zhang et al. 2013; Xing et al. 2020). As shown in Fig. 3c, the adsorption amount of CuO on MB in acidic condition was worse than that in alkaline conditions. Moreover, under alkaline condition, the reaction between OH^- and $SO_4{\cdot}^-$ and the self-consumption of ·OH may decrease the degradation performance of MB (Eq. 1 and 2) (Guan et al. 2011; Liang and Su 2009).

$$SO_4\bullet^- + OH^- \rightarrow \bullet OH + SO_4^{2-} \quad (1)$$

$$\bullet OH + \bullet OH \rightarrow H_2O_2 \quad (2)$$

$$SO_4\bullet^- + S_2O_8^{2-} \rightarrow SO_4^{2-} + S_2O_8\bullet^- \quad (3)$$

$$\bullet OH + S_2O_8^{2-} \rightarrow OH^- + S_2O_8\bullet^- \quad (4)$$

To discuss the effect of PS concentration on oxidation reaction, the degradation effect of MB with PS at different concentrations were studied. As shown in Fig. 2b, less than 10% MB was adsorbed by copper oxide. When PS concentration was kept between 0 and 2.0 g/L, MB degradation efficiency significantly increased as PS concentration increased.

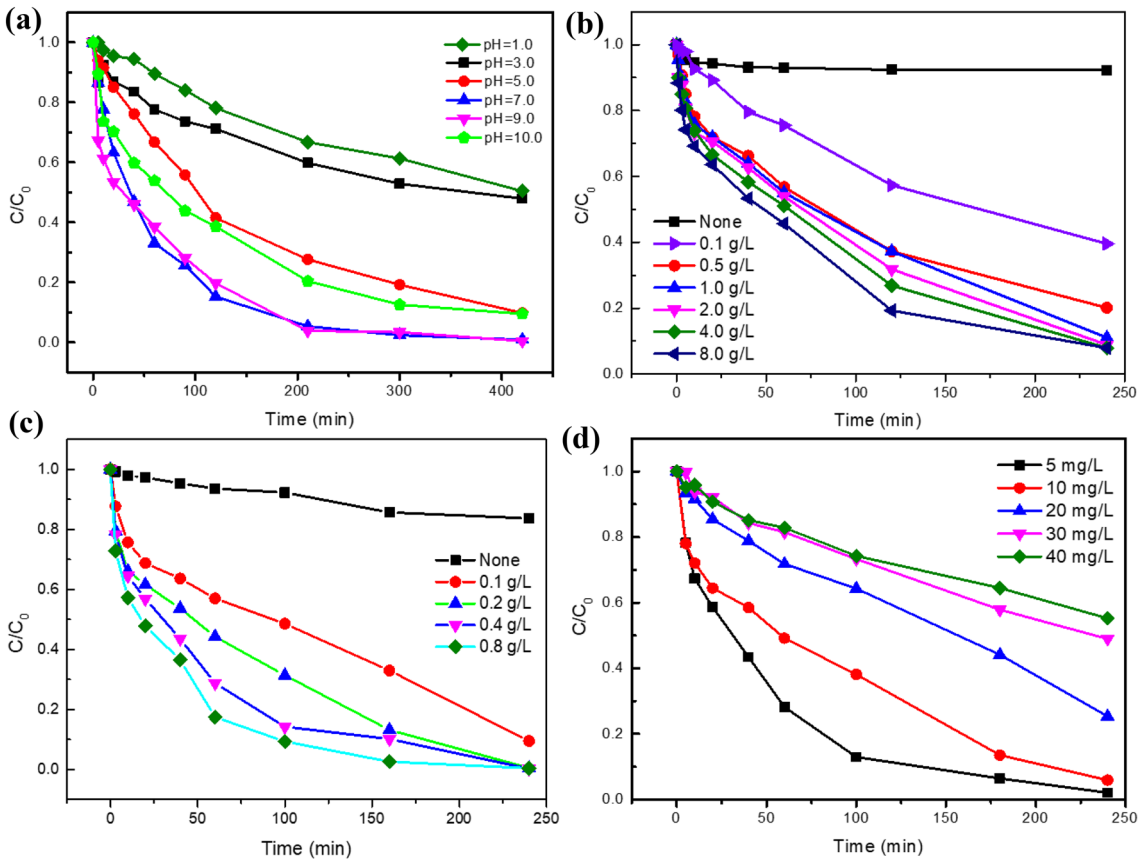

Fig. 2 Effect of (**a**) initial pH; (**b**) PS dosage; (**c**) CuO dosage; (**d**) concentration of MB on the degradation efficiency of MB (Reaction conditions: [CuO] = 0.2 g/L, [PS] = 2.0 g/L, [MB] = 10 mg/L, T = 25℃, initial pH of **b**, **c**, **d** = 6.3)

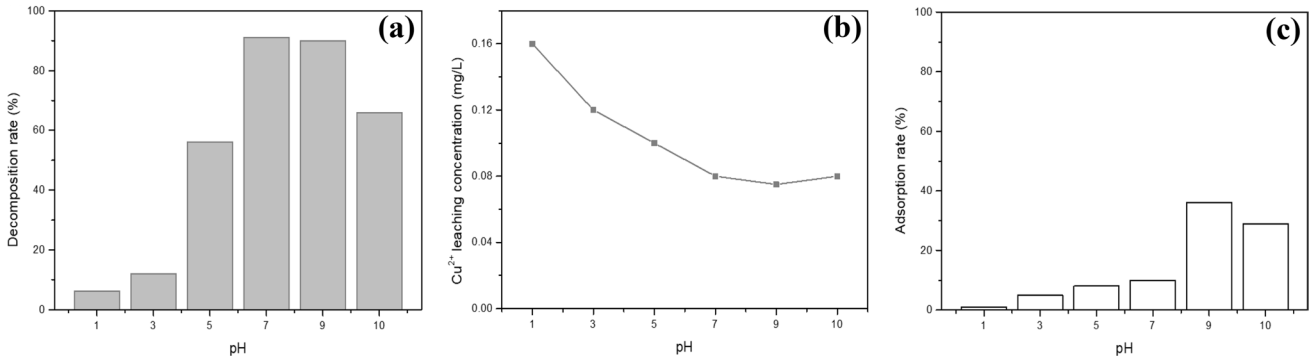

Fig. 3 **a** Decomposition rate (%) of PS, **b** Cu^{2+} leaching, and **c** adsorption of MB on CuO at the different initial solution pH ([CuO] = 0.2 g/L, [MB] = 10 mg/L, T = 25 ℃)

The maximum degradation efficiency was more than 90% at 2.0 g/L. When PS concentration exceeded 2.0 g/L, the degradation efficiency could not increase anymore, which could be explained by the radical interactions as a result of the excessive $SO_4\cdot-$ generation (Eqs. 3 and 4) (Monteagudo et al. 2018). Therefore, the suitable concentration of PS was 2.0 g/L.

The effect of CuO dosage on MB degradation was studied. The degradation rate of MB was less than 20% after 4 h without CuO catalysts (Fig. 2c), indicating that MB was hardly degraded by PS directly. According to the literature, the oxidation potential of $SO_4\cdot-$ was 2.6 V, while that of $S_2O_8^{2-}$ was only 2.01 V, which was significantly lower than $SO_4\cdot-$ (Zhou et al. 2013). The addition of CuO can effectively promote the degradation of MB. The degradation efficiency of MB gradually increased as the dosage of CuO increased from 0.1 to 0.2 g/L. However, further addition of copper oxide had little effect on the degradation efficiency. The possible reason was that excessive CuO generated more free radicals, causing quenched reactions between themselves (Fang et al. 2015). Therefore, 0.2 g/L was adopted as the optimum dosage of CuO.

To explore the influence of MB concentration on degradation effect in the reaction system, the degradation properties of MB with different concentration was investigated. It can be seen from Fig. 2d that when CuO dosage was 0.2 g/L, degradation efficiency decreased as MB initial concentration increased. Meanwhile, it took more time to achieve similar removal efficiency when the MB concentration was higher than 10 mg/L. The same results could be found in Fig. S1. In the degradation process, it will generate a purple floc, which was gradually disappeared as the increasing time. This phenomenon has been observed in another study (Ghauch et al. 2012b). It would take 80 min to decolorize 10 mg/L MB, while the solution became colorless as the reaction lasted for 250 min when the MB concentration was 40 mg/L. In further experiment, 10 mg/L was selected as the pollutant concentration without special emphasis.

Dye wastes contain a variety of pollutants. Generally, most of them are salt substances, such as NaCl, Na_2SO_4, and $NaHCO_3$. These salts may affect the degradation efficiency. They would directly participate in the reaction to generate the intermediate products or inhibitory oxidants, catalysts (Chan and Chu 2009). Figure 4a shows the effect of different concentrations of NaCl on MB degradation in the system. The results showed that NaCl basically did not have any adverse effect on this catalytic reaction, which was consistant with the results in removal of ciprofloxacin by persulfate activation with CuO (Xing et al. 2020). Figure 4b shows the effect of different concentrations of Na_2SO_4 on the reaction in the system. The addition of Na_2SO_4 imposed significantly inhibitive effect on the reaction. The inhibitions caused by Na_2SO_4 could be attributed to the decrease of the oxidation reduction potential (ORP) of $SO_4\cdot^-/SO_4^{2-}$. A high Na_2SO_4 concentration could decrease the ORP of $SO_4\cdot^-/SO_4^{2-}$, and lead to less efficient activation of PS. Figure 4c shows the effect of $NaHCO_3$ on the degradation of MB. The removal of MB was greatly inhibited in the presence of $NaHCO_3$, which may be due to the fact that $NaHCO_3$ can react with PS to produce new compounds, thus affecting the generation of sulfate radicals. Lei et al. (2015) proposed that PS can react with bicarbonate to generate peroxymono-carbonate (Eq. 5), and the conversion of Cu^{2+} into Cu^{3+} can be accelerated without relying on PS (Eq. 6). Other study also confirmed that the addition of $NaHCO_3$ can boost catalytic degradation of Acid Red 1 in CuO-CFs/PMS system. The possible reason was that $NaHCO_3$ reduced Cu^{2+} overflow and generated more active groups, which accelerated the degradation reaction (Yang et al. 2017). In this experiment, the high-concentrated $NaHCO_3$ obviously had an inhibitive effect on the reaction, this phenomenon may be due to the free radical capture effect of HCO_3^- itself (Eqs. 7 and 8), and reaction efficiency was reduced.

$$S_2O_8^{2-} + HCO_3^- \rightarrow SO_3^- + SO_4^- + HCO_4^- \quad (5)$$

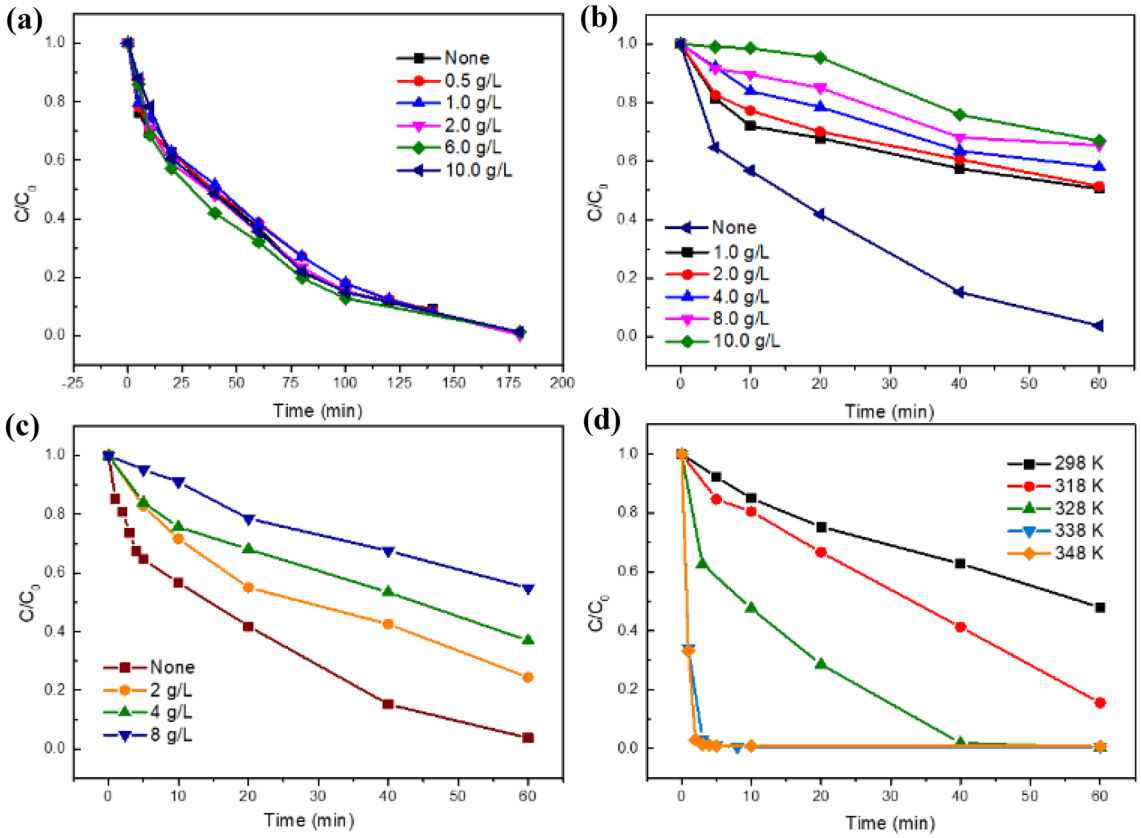

Fig. 4 Effect of **a** NaCl, **b** Na_2SO_4, **c** $NaHCO_3$, and **d** temperature on the degradation of MB (Reaction conditions: [CuO] = 0.2 g/L, [MB] = 10 mg/L, [PS] = 2 g/L, initial pH = 6.3)

$$S_2O_8^{2-} + Cu^{2+} \rightarrow SO_4 \bullet^- + SO_4^{2-} + Cu^{3+} \quad (6)$$

$$\bullet OH + HCO_3^- \rightarrow CO_3 \bullet^- + H_2O \quad (7)$$

$$SO_4 \bullet^- + HCO_3^- \rightarrow SO_4^{2-} + HCO_3 \bullet^- \quad (8)$$

The temperature has played an important role in the rate of catalyzed reaction. To explore the effect of temperature on the catalyzed reaction system, different temperatures were adopted in the experiment, as shown in Fig. 4d. The degradation efficiency was enhanced as the system temperature increased, which was ascribed to more PS decomposition under higher temperatures (Huang et al. 2002). When the reaction system reached 338 K, 10 mg/L MB solution can be removed within 3 min. Therefore, the removal efficiency of MB was significantly improved by increasing the temperature.

The Activation Energy

To study the energy needed by catalytic degradation of MB with CuO/PS system, the pseudo-first-order kinetic equation was used to fit the reaction process (Saputra et al. 2014). The formulas were presented in Supporting Information (Text S1). The degradation of CuO/PS system on MB followed pseudo-first-order kinetic model, k_{obs} magnified with the reaction temperature increase with the same MB concentration (Table S1). At the same time, ln k_{obs} were fitted to 1/T, which was shown in Fig. 5. The reaction activation energy (E_A) was obtained through Eqs. 11 and 12 (Supporting Information). When MB concentration was 10 mg/L, E_A needed by CuO catalyst to catalyze and degrade MB was 137.8 kJ/mol. The E_A values was lower than that obtained for BPA degradation (184.00 kJ/mol) in the heat-activated (Qi et al. 2017).

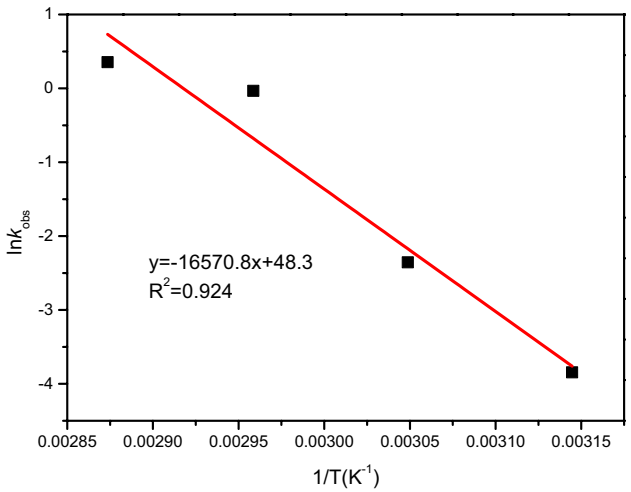

Fig. 5 The linear relationship of ln k_{obs} vs. 1/T for the degradation reaction of MB in CuO/PS system (Reaction conditions: [CuO] = 0.2 g/L, [MB] = 10 mg/L, [PS] = 2 g/L, T = 25 ℃, initial pH = 6.3)

Mechanistic Insights

To confirm the occurrence of radicals involved in the reactions, chemical quenching experiments were designed at first. Methanol (MeOH), *t*-butanol (TBA) were adopted to determine the free radicals in the systems containing SO_4·− and ·OH (Wang et al. 2015; Ye et al. 2017). *P*-benzoquinone (BQ) and furfuryl alcohol (FFA) were also used to estimate if $^1O_2$ and O_2·− participate in the reaction (Li et al. 2018b; Yang et al. 2019). As shown in Fig. 6a, the removal efficiency was decreased by adding MeOH and TBA, which suggested that there were SO_4·− and ·OH free radicals in this reaction system. When adding MeOH, the reduced amplitude of the reaction was greater than adding TBA. The phenomenon revealed that the radical quenching effect of EtOH was higher than that of TBA, which indicated that SO_4·− played a more important role in the process (Xie et al. 2015). Moreover, EPR spectroscopy was employed to monitor the evolution of reactive radicals in the PS/CuO system. The EPR tests were carried out using DMPO, TEMP as the spin trapping agent (Qi et al. 2016). As shown in Fig. 6b, the signal of the DMPO-OH· and DMPO-SO_4· adduct was detected and the signal has lasted for 30 min. The results also showed that SO_4· played a more significant role in the degradation of MB.

The addition of BQ had little effect on the degradation of MB, indicating the effect of superoxide radical on the reaction was weak. When FFA was added, the degradation of MB was significantly inhibited, implying the key role of $^1O_2$ in this process. To further clarify the mechanism of PS activation with CuO, TEMP was used to trap singlet oxygen with the formation of spin-adduct TEMPO. As shown in Fig. 6c, the signal of TEMP adduct generated by $^1O_2$ oxidation was observed in the systems, and its intensity remained stable in 30 min reaction time. It further proved that singlet oxygen played an important role in the reaction.

Application Properties

Catalyst stability was directly associated with the catalyst application potential, so the reuse and stability of catalysts were discussed (Xia et al. 2017). Figure 7a shows the diagram for the degradation of MB with PS activated by CuO repeatedly. After two cycles, the efficiency of catalyzed degradation was slightly decreased. After five consecutive batches of catalysts, approximately 70% removal rate was achieved. The decreased activity was probably attributed to the adsorption of reaction intermediates on the catalyst surface. The active sites of the catalyst were occupied

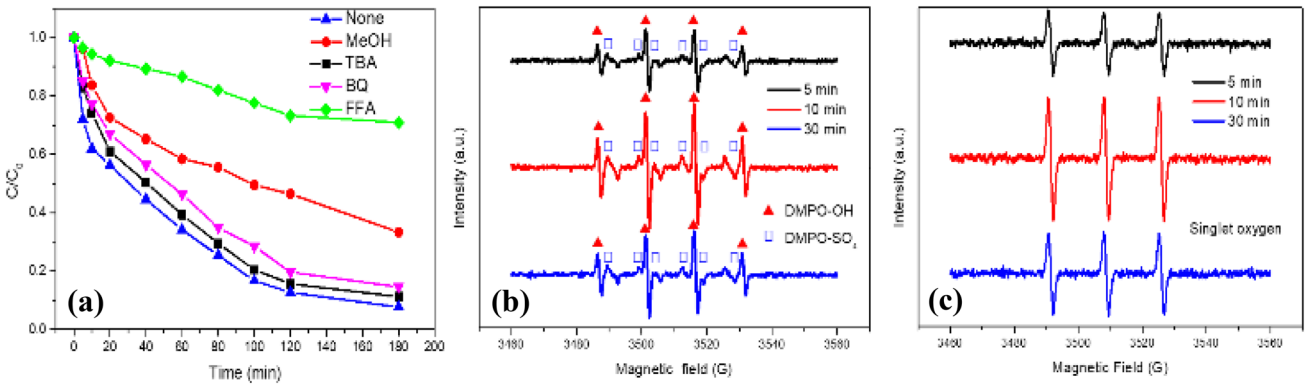

Fig. 6 The degradation of MB using CuO/PS system in the presence of **a** MeOH, TBA, BQ and FFA (Reaction conditions: [CuO] = 0.2 g/L, [MB] = 10 mg/L, [PS] = 2 g/L, [MeOH] = 250 mmol/L, [TBA] = 250 mmol/L, [BQ] = 100 mmol/L, [FFA] = 100 mmol/L, T = 25 ℃, initial pH = 6.3), DMPO spin-trapping EPR spectra (**b**) and TEMP spin-trapping EPR spectra (**c**) of CuO/PS system (reaction conditions: [CuO] = 0.2 g/L, [PS] = 2 g/L, [MB] = 10 mg/L, T = 25 ℃, initial pH = 6.3)

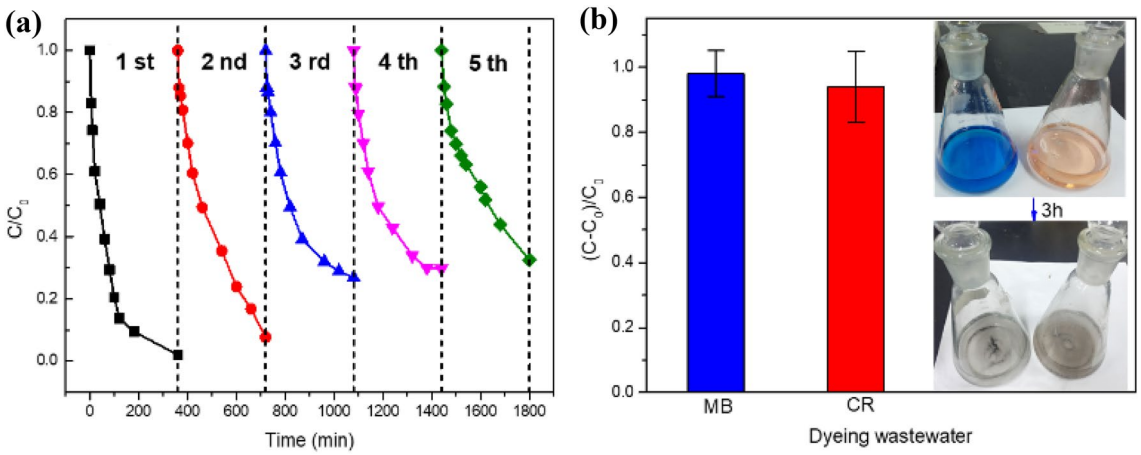

Fig. 7 **a** The degradation of MB using CuO/PS system for five cycles (Reaction conditions: [CuO] = 0.2 g/L, [PS] = 2 g/L, [MB] = 10 mg/L, T = 25 ℃, initial pH = 6.3); **c** The degradation of dyeing wastewater using CuO/PS system (reaction conditions: [CuO] = 0.4 g/L, [PS] = 3 g/L, [MB] = 10 mg/L, [CR] = 10 mg/L, [NaCl] = 4 g/L, [$NaHCO_3$] = 4 g/L, T = 25 ℃, initial pH = 6.1)

and impaired. Meanwhile, the catalyst was sped up Cu^{2+} overflow and the concentration of Cu^{2+} in the cycle process was also monitored. With the continuous reaction batch, the overflow amount of Cu^{2+} gradually increased, as shown in Fig. S2. After fifth recycling, the leached Cu^{2+} was 0.17 mg/L, which was lower than the drinking water standard of 1.3 mg/L set by U.S EPA (Lei et al. 2015). These results indicated that the catalyst had good stability. Simulated MB and Congo Red (CR) textile wastewater containing NaCl (4 g/L), $NaHCO_3$ (4 g/L) were applied to testing the catalyst performance. The degradation performance of simulated textile wastewater was shown in Fig. 7b. The two kinds of wastewater can be completely decolorized and degraded in 3 h, which also indicated the potential application of CuO in textile wastewater treatment.

Conclusions

CuO catalyst prepared by the hydrothermal method can effectively activate PS to degraded methylene blue (MB). The optimum conditions for MB degradation were as follows: the dosage of CuO was 0.2 g/L, the concentration of PS was 2.0 g/L, and the pH was 7.0–9.0. The removal efficiency of MB was significantly improved by increasing the temperature. Cl^- has little effect on dye removal, but SO_4^{2-} and HCO_3^- have significant inhibitive effects on the catalytic performance. $SO_4\cdot-$ and $^1O_2$ should be the main reactive species for MB degradation. After the continuous five catalytic batches, its degradation can still reach about 70%. The excellent stability and degradation performance for simulated textile wastewater indicated CuO/PS system has the potential application for dyeing wastewater treatment.

Acknowledgements We gratefully acknowledge the generous support provided by the "National Natural Science Foundation of China (51908432)", the "Support Program from the Central Government for the Local Science and Technology Development of Hubei Province (2019ZYYD068, 2018ZYYD024)", and the "Natural Science Foundation of Hubei Province (2018CFB397)," China.

Data Availability Statement All data, models, and code generated or used during the study appear in the submitted article.

References

Ahmad M, Teel AL, Watts RJ (2013) Mechanism of persulfate activation by phenols. Environ Sci Technol 47:5864–5871

Anipsitakis GP, Dionysiou DD (2014) Radical generation by the interaction of transition metals with common oxidants. Environ Sci Technol 38:3705–3712

Chan KH, Chu W (2009) Degradation of atrazine by cobalt-mediated activation of peroxymonosulfate: Different cobalt counteranions in homogenous process and cobalt oxide catalysts in photolytic heterogeneous process. Water Res 43:2513–2521

Chen Y, Yan J, Ouyang D, Qian L, Han L, Chen M (2017) Heterogeneously catalyzed persulfate by CuMgFe layered double oxide for the degradation of phenol. Appl Catal A-Gen 538:19–26

Damasceno BS, Silva AFV, Araújo ACV (2020) Dye adsorption onto magnetic and superparamagnetic Fe_3O_4 nanoparticles: a detailed comparative study. J Environ Chem Eng 8:103994

Dotto J, Fagundes-Klen MR, Veit MT, Palácio SM, Bergamasco R (2019) Performance of different coagulants in the coagulation/flocculation process of textile wastewater. J Clean Prod 208:656–665

Drzewicz P, Perez-Estrada L, Alpatova A, Martin J, Gamal EI-Din M (2012) Impact of peroxydisulfate in the presence of zero valent iron on the oxidation of cyclohexanoic acid and naphthenic acids from oil sands process-affected water. Environ Sci Technol. 46:8984–8991

Du X, Zhang Y, Hussain I, Huang S, Huang W (2017) Insight into reactive oxygen species in persulfate activation with copper oxide: activated persulfate and trace radicals. Chem Eng J 313:1023–1032

Fang G, Liu C, Gao J, Dionysiou D, Zhou D (2015) Manipulation of persistent free radicals in biochar to activate persulfate for contaminant degradation. Environ Sci Technol 49:5645–5653

Feng Y, Zhou H, Liu G, Qiao J, Wang J, Lu H, Yang L, Wu Y (2012) Methylene blue adsorption onto swede rape straw (*Brassica napus* L.) modified by tartaric acid: equilibrium, kinetic and adsorption mechanisms. Bioresour Technol. 125:138–144

Florenza X, Solano AMS, Centellas F, Martínez-Huitle CA, Brillas E, Garcia-Segura S (2014) Degradation of the azo dye Acid Red 1 by anodic oxidation and indirect electrochemical processes based on Fenton's reaction chemistry. Relationship between decolorization, mineralization and products. Electrochim Acta 142:276–288

Furman OS, Teel AL, Watts RJ (2010) Mechanism of base activation of persulfate. Environ Sci Technol 44:6423–6428

Ghauch A, Tuqan AM, Kibbi N (2012) Ibuprofen removal by heated persulfate in aqueous solution: a kinetics study. Chem Eng J 197:483–492

Ghauch A, Tuqan AM, Kibbi N, Geryes S (2012) Methylene blue discoloration by heated persulfate in aqueous solution. Chem Eng J 213:259–271

Guan YH, Ma J, Li XC, Fang JY, Chen LW (2011) Influence of pH on the formation of sulfate and hydroxyl radicals in the UV/Peroxymonosulfate system. Environ Sci Technol 45:9308–9314

He Y, Li G, Wang H, Zhao J, Su H, Huang Q (2008) Effect of operating conditions on separation performance of reactive dye solution with membrane process. J Membr Sci 321:183–189

Hu P, Long M (2016) Cobalt-catalyzed sulfate radical-based advanced oxidation: a review on heterogeneous catalysts and applications. Appl Catal B 181:103–117

Hu M, Zheng S, Mi B (2016) Organic fouling of graphene oxide membranes and its implications for membrane fouling control in engineered osmosis. Environ Sci Technol 50:685–693

Huang KC, Couttenye RA, Hoag GE (2002) Kinetics of heat-assisted persulfate oxidation of methyl tert-butyl ether (MTBE). Chemosphere 49:413–420

Huang L, Zhang L, Li D, Xin Q, Jiao R, Hou X, Zhang Y, Li H (2020) Enhanced phenol degradation at near neutral pH achieved by core-shell hierarchical 4A zeolite/Fe@Cu catalyst. J Environ Chem Eng 8:103933

Ji F, Li C, Deng L (2011) Performance of CuO/Oxone system: heterogeneous catalytic oxidation of phenol at ambient conditions. Chem Eng J 178:239–243

Johnson RL, Tratnyek PG, Johnson RO (2008) Persulfate persistence under thermal activation conditions. Environ Sci Technol 42:9350–9356

Lei Y, Chen CS, Tu YJ, Huang YH, Zhang H (2015) Heterogeneous degradation of organic pollutants by persulfate activated by CuO–Fe_3O_4: mechanism, stability, and effects of pH and bicarbonate ions. Environ Sci Technol 49:6838–6845

Li Q, Pan F, Li W, Li D, Xu H, Xia D, Li A (2018) Enhanced adsorption of bisphenol A from aqueous solution with 2-vinylpyridine functionalized magnetic nanoparticles. Polymers 10:1136

Li H, Shan C, Pan B (2018) Fe(III)-doped g-C_3N_4 mediated peroxymonosulfate activation for selective degradation of phenolic compounds via high-valent iron-oxo species. Environ Sci Technol 52:2197–2205

Li Q, Wang M, Yuan X, Li D, Xu H, Sun L, Pan F, Xia D (2019) Study on the adsorption and desorption performance of magnetic resin for Congo red. Environ Technol. https://doi.org/10.1080/09593330.2019.1673830

Liang C, Su HW (2009) Identification of sulfate and hydroxyl radicals in thermally activated persulfate. Ind Eng Chem Res 48:5558–5562

Liang HY, Zhang YQ, Huang SB, Hussain I (2013) Oxidative degradation of *p*-chloroaniline by copper oxidate activated persulfate. Chem Eng J 218:384–391

Liu C, Shih K, Sun CX, Wang F (2012) Oxidative degradation of propachlor by ferrous and copper ion activated persulfate. Sci Total Environ 416:507–512

Liu S, Huang J, Ye Y, Zhang A, Pan L, Chen X (2013) Microwave enhanced Fenton process for the removal of methylene blue from aqueous solution. Chem Eng J 215–216:586–590

Liu J, Wu P, Yang S, Rehman S, Ahmed Z, Zhu N, Dang Z, Liu Z (2020) A photo-switch for peroxydisulfate non-radical/radical activation over layered CuFe oxide: rational degradation pathway choice for pollutants. Appl Catal B 261:118232

Ma Q, Zhang H, Zhang X, Li B, Guo R, Cheng Q, Cheng X (2019) Synthesis of magnetic CuO/$MnFe_2O_4$ nanocompisite and its high activity for degradation of levofloxacin by activation of persulfate. Chem Eng J 360:848–860

Monteagudo JM, El-Taliawy H, Durán A, Caro G, Bester K (2018) Sono-activated persulfate oxidation of diclofenac: degradation, kinetics, pathway and contribution of the different radicals involved. J Hazard Mater 357:457–465

Oh WD, Dong Z, Lim TT (2016) Generation of sulfate radical through heterogeneous catalysis for organic contaminants removal: current development, challenges and prospects. Appl Catal B 194:169–201

Oliveira-Cruz FS, Nascimento MA, Puiatti GA, Oliveira AF, Mounteer AH, Lopes RP (2020) Textile effluent treatment using a fixed bed reactor using bimetallic Fe/Ni nanoparticles supported on chitosan spheres. J Environ Chem Eng 8:104133

Qi C, Liu X, Ma J, Lin C, Li X, Zhang H (2016) Activation of peroxymonosulfate by base: implications for the degradation of organic pollutants. Chemosphere 151:280–288

Qi C, Liu X, Lin C, Zhang H, Li X, Ma J (2017) Activation of peroxymonosulfate by microwave irradiation for degradation of organic contaminants. Chem Eng J 315:201–209

Qin Y, Li G, Gao Y, Zhang L, Sik-Ok Y, An T (2018) Persistent free radicals in carbon-based materials on transformation of refractory organic contaminants (rocs) in water: a critical review. Water Res 137:130–143

Saputra E, Muhammad S, Sun H, Ang H, Tadé M, Wang S (2014) Shape-controlled activation of peroxymonosulfate by single crystal α-Mn_2O_3 for catalytic phenol degradation in aqueous solution. Appl Catal B 154–155:246–251

Sayğılı H, Güzel F (2016) High surface area mesoporous activated carbon from tomato processing solid waste by zinc chloride activation: process optimization, characterization and dyes adsorption. J Clean Prod 113:995–1004

Sayğılı H, Güzel F, Önal Y (2015) Conversion of grape industrial processing waste to activated carbon sorbent and its performance in cationic and anionic dyes adsorption. J Clean Prod 93:84–93

Vijayaraghavan G, Sivakumar T, Kumar AV (2011) Application of plant based coagulants for wastewater treatment. Int J Adv Eng Res Stud 1:88–92

Wacławek S, Lutze H, Grübel K, Padil V, Černík M, Dionysiou DD (2017) Chemistry of persulfates in water and wastewater treatment: a review. Chem Eng J 330:44–62

Wang J, Wang S (2018) Activation of persulfate (PS) and peroxymonosulfate (PMS) and application for the degradation of emerging contaminants. Chem Eng J 334:1502–1517

Wang Y, Sun H, Ang HM, Tadé M, Wang S (2015) 3D-hierarchically structured MnO_2 for catalytic oxidation of phenol solutions by activation of peroxymonosulfate: Structure dependence and mechanism. Appl Catal B 164:159–167

Wang J, Yang M, Liu R, Hu C, Liu H, Qu J (2019) Anaerobically-digested sludge conditioning by activated peroxymonosulfate: Significance of EDTA chelated-Fe^{2+}. Water Res 160:454–465

Xia D, Li Y, Huang G, Yin R, An T, Li G, Zhao H, Lu A, Wong PK (2017) Activation of persulfates by natural magnetic pyrrhotite for

water disinfection: efficiency, mechanisms, and stability. Water Res 112:236–247
Xie P, Ma J, Liu W, Zou J, Yue S, Li X, Wiesner M, Fang J (2015) Removal of 2-MIB and geosmin using UV/persulfate: contributions of hydroxyl and sulfate radicals. Water Res 69:223–233
Xing S, Li W, Liu B, Wu Y, Gao Y (2020) Removal of ciprofloxacin by persulfate activation with CuO: a pH dependent mechanism. Chem Eng J 382:122837
Yang S, Yang X, Shao X, Niu R, Wang L (2011) Activated carbon catalyzed persulfate oxidation of azo dye acid orange 7 at ambient temperature. J Hazard M 186:659–666
Yang Z, Dai D, Yao Y, Chen L, Liu Q, Luo L (2017) Extremely enhanced generation of reactive oxygen species for oxidation of pollutants from peroxymonosulfate induced by a supported copper oxide catalyst. Chem Eng J 322:546–555
Yang Z, Qian J, Yu A, Pan B (2019) Singlet oxygen mediated iron-based Fenton-like catalysis under nanoconfinement. P N A S 116:6659–6664
Ye Y, Jiang Z, Xu Z, Zhang X, Wang D, Lv L, Pan N (2017) Efficient removal of Cr(III)-organic complexes from water using UV/Fe(III) system: negligible Cr(VI) accumulation and mechanism. Water Res 126:172–178
Yu J, Tang L, Pang Y, Zeng G, Feng H, Zou J, Wang J, Feng C, Zhu X, Ouyang X, Tan J (2020) Hierarchical porous biochar from shrimp shell for persulfate activation: a two-electron transfer path and key impact factors. Appl Catal B 260:118160
Zhan Y, Wan X, He S, Yang Q, He Y (2018) Design of durable and efficient poly (arylene ether nitrile)/bioinspired polydopamine coated graphene oxide nanofibrous composite membrane for anionic dyes separation. Chem Eng J 333:132–145
Zhang T, Zhu H, Croué JP (2013) Production of sulfate radical from peroxymonosulfate induced by a magnetically separable $CuFe_2O_4$ spinel in water: efficiency, stability, and mechanism. Environ Sci Technol 47:2784–2791
Zhang T, Chen Y, Wang Y, Le Roux J, Yang Y, Croué J (2014) Efficient peroxydisulfate activation process not relying on sulfate radical generation for water pollutant degradation. Environ Sci Technol 48:5868–5875
Zhou L, Zheng W, Ji Y, Zhang J, Zeng C, Zhang Y, Wang Q, Yang X (2013) Ferrous-activated persulfate oxidation of arsenic(III) and diuron in aquatic system. J Hazard M 263:422–430